Pattern of Hydroxyapatite Crystal Growth on Bleached Enamel Following the Application of Two Antioxidants: An Atomic Force Microscope Study

Chitra P Bhusari*/ Divya S Sharma**

Objectives: *This study observed the topographical pattern of hydroxyapatite deposition and growth (D&G) on bleached enamel following application of two antioxidants (sodium ascorbate and catalase) using atomic force microscope.* ***Study design:*** *Twenty enamel specimens (4×3×2mm), prepared from extracted impacted third molars, were mounted in self-cure acrylic and randomly grouped as: Group I-untreated; Group II- 35%H_2O_2 ; Group III- 35%H_2O_2 + artificial saliva; Group IV- 35%H_2O_2 + catalase+ artificial saliva; Group V- 35%H_2O_2 + sodium ascorbate+ artificial saliva. Groups I and II were observed immediately after treatment. Groups III-V were observed after 72 hrs. Roughness average was also calculated and analyzed with non-parametric Kruskall-Wallis ANOVA and Mann-Whitney tests.* ***Results:*** *H_2O_2 dissolved matrix, exposed hydroxyapatite crystals (HACs), causing dissolution on the sides of and within HACs and opening up of nano-spaces. Artificial saliva showed growth of dissoluted crystals. Antioxidants+saliva showed potentiated remineralization by D&G on dissoluted HACs of bleached enamel. Catalase potentiated block-shaped, while sodium ascorbate the needle-shaped crystals with stair-pattern of crystallization. Evidence of oxygen bubbles was a new finding with catalase. Maximum roughness average was in group V followed by group II > group IV > group III > group I.* ***Conclusion:*** *Post-bleaching application of catalase and sodium ascorbate potentiated remineralization by saliva, but in different patterns. None of the tested antioxidant could return the original topography of enamel.*

Key words: atomic force microscope, antioxidants, catalase, dental bleaching, sodium ascorbate

From the Department of Pediatric and Preventive Dentistry
Modern Dental College and Research Centre, Indore, India.
*Chitra P Bhusari, MDS, Senior Lecturer.
**Divya S Sharma, MDS, Professor and Head.

Send all correspondence to
Divya S Sharma,
Dept. of Pediatric and Preventive Dentistry
Modern Dental College and Research Centre
Gandhi Nagar, Airport road
Indore (MP), India
Phone: +91 9977701098
E mail: drdivyassharma@gmail.com

INTRODUCTION

Bleaching is a conservative treatment alternative for discolored teeth, be it at-home or in-office[1] and popular among young children[2] as well. Hydrogen peroxide (H_2O_2) containing bleaching products, despite being benign causes sensitivity, susceptibility for plaque accumulation, abrasive wear, and reduced microhardness.[3-5] However, as the results of bleaching obtained are unstable, repeated treatment would add to the adverse effects. Many researchers observed altered rough surface morphology of bleached enamel, having deep gaps providing channels for penetration of H_2O_2.[6-8] Efeoglu *et al* [9] found enamel demineralization up to 50µm below the enamel surface with 10% carbamide peroxide. In-office bleach with concentrated H_2O_2 can penetrate the pulp chamber within 10 minutes, and is a possible cause of sensitivity.[10,11] Accordingly, Bistey *et al* [12] suggested repeated but shortened bleaching time as all side effects tend to resolve after 2-3 weeks, while saliva remineralizes the tooth surface.

Nonetheless during this period of mineral gain and return of microhardness, bleached teeth remain predisposed to adverse effects. Incomplete remineralization of bleached

enamel with artificial saliva is prone to abrasive wear and decalcification.[13] Reduced bond strength and microhardness of enamel are added problems with bleaching procedure.[5, 13, 14] More chances of H_2O_2 penetration are there in children with deciduous or young permanent teeth. Therefore not only reversal of bond strength but also better remineralization and minimization of health hazards is of prime importance in children and adolescents.

There is generation of radicals during bleaching.[15-17] Presence of reactive oxygen species (ROS) on bleached enamel surface is thought responsible for various adverse effects. Nonetheless authors found varying reversal of bond strength with different antioxidant application following bleaching. [14, 18-22] A few studies compared pre and post-bleaching enamel effects using scanning electron microscope (SEM) or atomic force microscope (AFM).[6-8, 23-24] Kwon KY *et al* [25] stated that on molecular level these processes are governed by pattern of hydroxyl apatite crystals (HACs) growth. Simmer and Fincham[26] had described that HACs grow anisotropically i.e. at different rates in different directions giving rise to 3 possible shapes (needle, block and plate shaped) depending on selective extension/inhibition of crystal faces. If it is true there may be differences in shapes of HACs deposited on bleached enamel following various antioxidants and remineralizing agents. To date, no study has observed surface topography revealing pattern of D&G of hydroxyapatite on bleached enamel or following antioxidant application. There lies a need of knowledge of topographical changes at molecular level following various chemical treatments for better understanding of biological process taking place at enamel/ bleaching agent; bleaching agent+saliva; antioxidant+saliva interfaces.

As there is no baseline study till now observing the crystal level topography of bleached enamel following various antioxidants, we undertook a preliminary study to observe effects of two natural antioxidants; one commonly studied i.e. sodium ascorbate (SA) and the other, a potent but less studied i.e. catalase on human enamel after in-office bleaching with 35% H_2O_2 gel. We hypothesize that application of antioxidant would remove the residual ROS facilitating remineralization and thus probably reverse the original topography of bleached enamel. Henceforth we opted for AFM to observe enamel topography.

MATERIALS AND METHOD

Prior approval for the study was obtained from Institutional ethical committee. Enamel specimens were prepared from freshly impacted permanent third molars because of the probable presence of aprismatic enamel and being free from physical and chemical influences of the oral cavity, thereby allowing unbiased inter-group comparison to begin with. The teeth were cleaned-off debris with a toothbrush. All teeth were inspected under stereomicroscope (Lawrence & Mayo, Bangalore, India) at 40× magnification for hypoplasia or cracks and teeth having such defects were excluded. Out of these, 30 teeth were disinfected with 0.1% thymol, then stored at -20°C[28] to rule out any effect of storing solution on enamel surface, owing to difference in mineral saturation of enamel and solution.

All teeth were defrosted for 4 h at room temperature. Enamel slabs (4×3×2mm) were prepared from the middle-third of the mesial aspect of molars using double-sided diamond disc (Keystone Industries, New Jersey, USA) to obtain flatter enamel. Samples were reinspected for any cracks under stereomicroscope at same magnification. Twenty six samples were embedded in autopolymerizing acrylic (Rapid Repair, Pyrax Polymer, Roorkee, India) discs of 1cm diameter exposing outer enamel only. To preserve natural enamel morphology, surface was not tampered. Twenty samples were then randomly grouped (table-1). All samples except Group I were bleached with Pola-Office tooth whitening system (Southern Dental Industries, Illinois, USA) for two 8 min consecutive applications and washed with distilled water. Group IV and V were subjected to a 5.5min (1/3rd of bleaching time)[14] application of respective antioxidants with cotton applicator, washed with distilled water for 30 sec and immersed in artificial saliva.[29]

Catalase powder (300mg) from bovine liver (Sigma-Aldrich, Missouri, USA; initial activity of 2000-5000 units/mg) was dissolved in 30ml of distilled water (10mg/ml = 20000-50000 units/mg) and stored at 4˚C as per the manufacturer's recommendation, until required. SA powder (Qualikems, New Delhi, India) (25gm), was mixed in 100ml distilled water (25% SA-solution).

Table 1- Distribution of group

Groups	Description
Group I	Untreated
Group II	35% H_2O_2 bleached
Group III	35% H_2O_2 bleached + artificial saliva
Group IV	35% H_2O_2 bleached + catalase + artificial saliva
Group V	35% H_2O_2 bleached + sodium ascorbate + artificial saliva

All specimens in groups III,IV and V were stored in artificial saliva for 72 hours prior to AFM evaluation (table-1). Artificial saliva (groups III, IV and V) was changed every day. The specimens in groups I &II were observed immediately.

Atomic force microscope (AIST-NT Inc., Novoto, California, model Smart SPM 1000) with Si cantilever (AIST-NT., NIIFP; dimension-3.6×1.6×0.4mm; R_{TIP}- 20 nm; resonant frequency- 118-190 kHz; force constant- 5,3 N/m) was used to image topography of enamel samples. Tip and sample distance was well maintained with vander-waal forces. Imaging was performed in semi-contact mode at room temperature (scan rate 1Hz; resolution 512×512 pixels) with resonant frequency of 152 kHz. AFM provides images with nanoscopic resolution in three dimensions (X, Y & Z) with added advantage that samples can be observed without surface tampering, in their hydrated state in open air at room temperature.

Furthermore roughness average (Ra) of surface was calculated using in-built IAPro software with the used AFM.

Data for Ra was tabulated and analyzed. Five groups had 4 samples each. Non- parametric test i.e. Kruskal-Wallis ANOVA was used to compare the mean of all the five groups.

Intergroup pair-wise comparison was done using Mann-Whitney Test (non-parametric test) to compare mean of two groups. SPSS for Windows version 18.0 was used for data analysis. Alpha was set at 0.05 and p-value less than 0.05 was considered statistically significant.

RESULTS

Surface topography of all the groups, deciphered under AFM is shown in figures 1-5. All 3D images were magnitude image (MI), while 2D images were any of the following- magnitude image (MI), phase image (PI) or height image (HI).

In group-I (Figure-1, a-b-c series) samples showed 3 distinctive patterns. *First pattern* (a1-5) revealed linearly arranged grains of HACs, oriented perpendicular to surface with linear grooves of varying depths. *Second pattern* (Figure-1, b1-5) revealed closely packed rod shaped HACs with 'c' face toward surface having isotropic growth on 'a' and 'b' face (thickness and width) with ~20nm long conical heads on 'c' face. No aprismatic enamel was visible in this sample, though freshly extracted impacted teeth were studied. *Third pattern* (c1-5) showed 4 dome shaped enamel prisms with interprismatic structure. HACs had 'c' face towards surface in middle of the prism while little apart and getting horizontally arranged with probably 'a' facets towards surface as they reach periphery especially in left lower prism.

Two distinctive patterns of severe topographic roughness were observed in Group-II (Figure-2, a-b series). *First pattern* (a1-5) showed opening up of nanospaces within and sides of crystals. *Second pattern* (b1-5) showed type-II etching pattern i.e. elevated heads of HA nanorods with dissoluted inter-crystal matrix.

In group-III (Figure-3, a-b series), images showed isolated areas of flat remineralization along with reduced groove depths. Figures a4-12 clearly displayed growth of pre-existed original and chemically injured HACs (in group II) along with some flat HACs. Similar pictures were there in another sample (b series) hence magnified views are not given.

Group-IV (Figure-4, a-b-c series) showed effective obliteration of craters and depressions (in group II) with different pattern of remineralization owing to different shapes of deposited HACs- a) a series showed block type HACs deposition. b) b-series showed many perpendicularly orientated rod shaped HACs along with overall even remineralization appearing in linear smooth plates. Many circular shallow smooth areas (CSSA) were observed (b 1-4). c) c series also showed plausible polycrystalline remineralization with many CSSA (red arrows, c1-3).

Group-V (Figure 5, a-b-c series) also showed potentiated remineralization. Four findings were common in all the series- a) stair-pattern remineralization, b) growth of needle

Figure-1(Group I, a-b-c series): a1-2- 2 distinct lines at right angle, the step (yellow arrow) and linear clefts (~.5-1µm, red arrow); densely packed, linear-perpendicular HACs. a3- Flat (yellow arrow) & rod shaped (red circle) HACs. a4- Deep valley (red arrow) and elevated rod-shaped perpendicular HACs. a5- Flat & elevated rod shaped HACs; Valleys as dark areas.

b1- Closely packed even heighted HACs. b2-3- Heads of closely packed HACs. b4-5- HACs with cone shaped heads, of good width and thickness with minimal amount of inter-rod matrix.

c1- Four prisms with interprismatic area; marked changed direction of HACs near periphery of prism. c2-3- Missing HACs in the middle of one prism; HACs are along the long axis of enamel rod. c4- Needle shaped HACs of uneven heights. c5- Magnified view of yellow rectangle in c1; the heads of HACs at different levels.

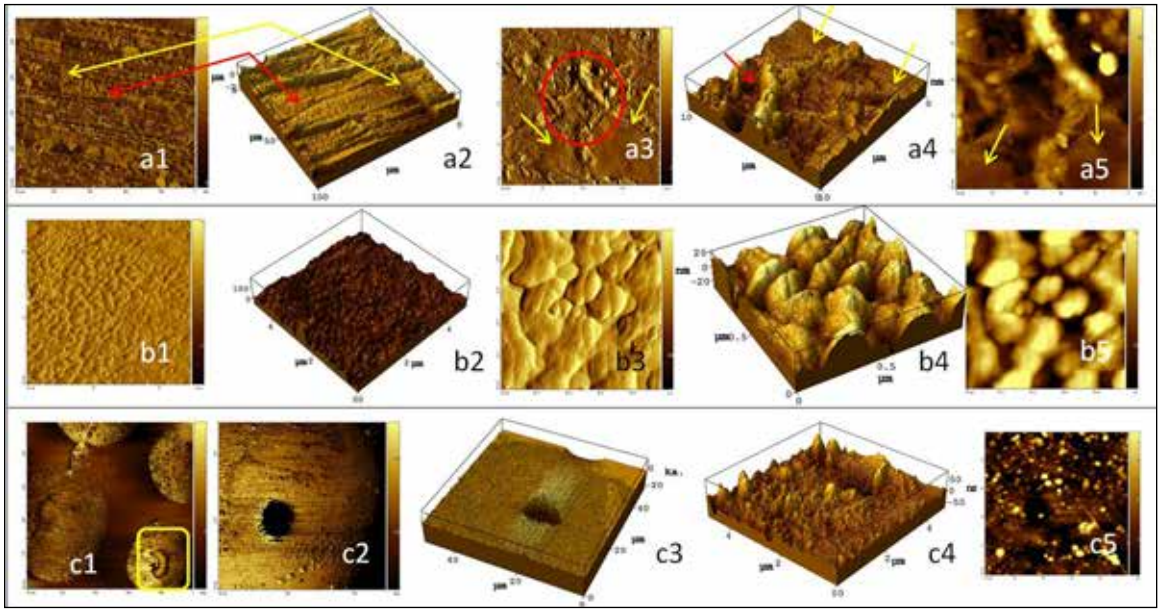

Figure 2 (Group II, a-b series); a1-2- Severe dissolution of organic matrix exposing partially dissoluted HACs in linear pattern. a3-4- Tiny heads of HACs, located in a grain; Margins of HACs are rough. a5- Heads of HACs at different levels; Encircled area in a3-4 is the deep valley here. b1-2 & b3-4(high resolution)- Type 2 etching pattern in centre of prism; At periphery changed direction of HACs (red arrow b1-4). b5- Opening up of inter-HAC spaces by their partial, lateral dissolution making their tiny heads appreciable.

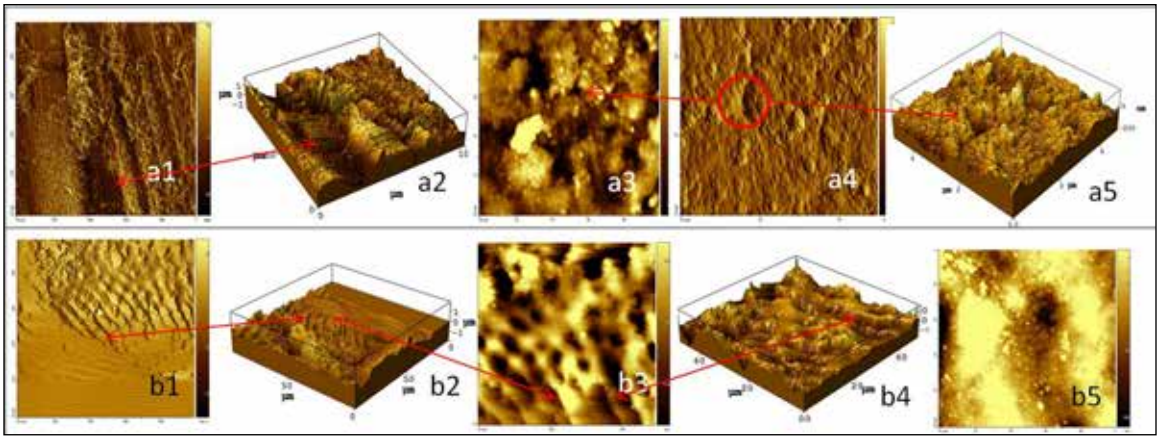

Figure 3 (Group III, a-b series); a1-2- Overall smooth surface, some flat HACs, craters, diagonally running shallow linear valleys (red arrows), clefts (broken red arrows) and elevations; Smooth crater and smooth area in a1 appear as deep crater(broken yellow arrow) and irregular flat crystals (yellow arrow) respectively in a2; Perpendicular deposition of HACs on upper right area. a3- Valleys in a1-2 (dark area here), running diagonally to the clefts in a2. Smooth crater in a1 (broken yellow arrow) are as dark areas. a4-6- Images show growth of injured HACs. a7-9- Rod shaped HACs deposition & growth (D&G) with one growing grain (red arrow); Flat HAC is correlated by red arrow. a10-12- Some coalesced dumbbell shaped HACs (red arrow).

b1-2- Steps, elevations (red arrows) & clefts (yellow arrow) on remineralizing surface; Three steps, appreciable in 3D only; Valleys, here too, running diagonally to clefts and steps.

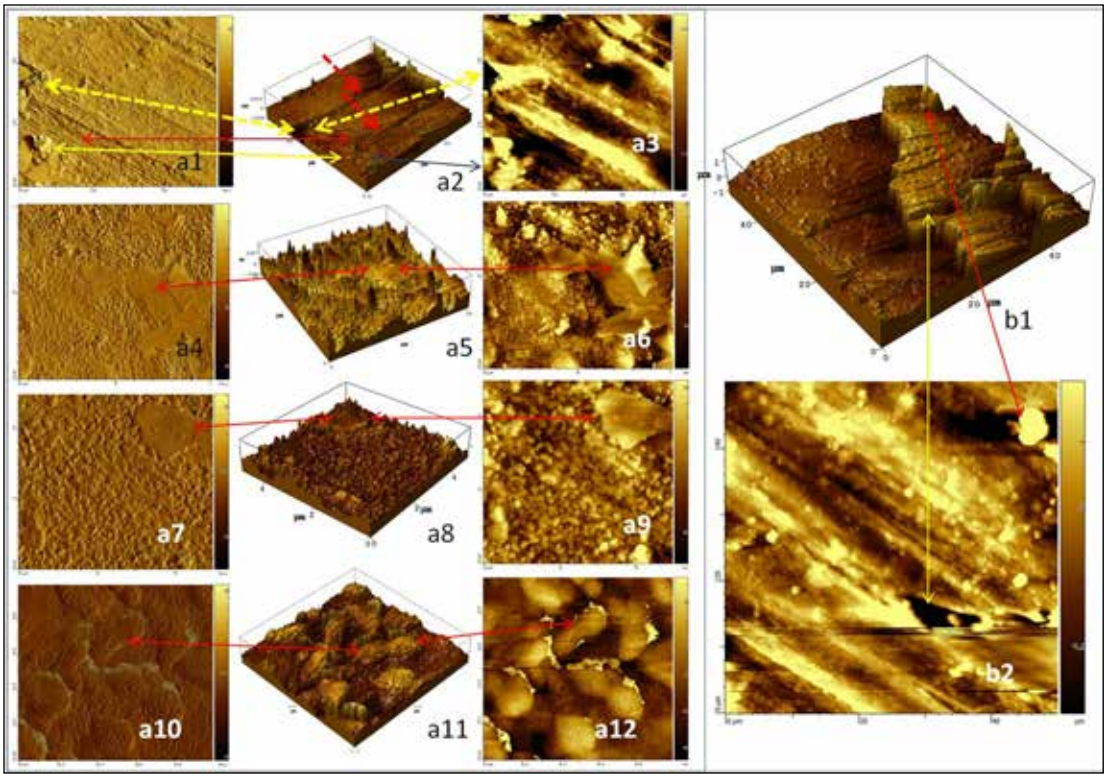

shaped HACs, c) horizontal surface of each stair was smooth, d) some horizontal surfaces were very smooth comprised of a parallel arrangement of closely packed needle shaped HACs of equal heights with good grain growth. In general flat crystals were not found except in very small areas of b-series in this group. Many findings were observed by correlating various images of AFM. Slightest depressions or elevations, not visible in 2D were identified in 3D or other images (e.g. Figure-5, b-3,7,8,9)

Mean Ra for group-I, II, III, IV and V was 1.352µm (±0.681), 2.249µm (±0.570), 1.676µm (±0.144), 1.895µm (±0.565), 2.458µm (±0.141) respectively *i.e.* R_a was not significant in any of the groups. Mean and intergroup comparison of Ra is shown in tables 2&3.

Figure 4 (Group IV, a-b-c series): a1- Plausible HACs and grain growth with linear elevations and shallow valleys (red arrow); Smooth area is with sparse HAC growth on it (black arrow). a2- Almost plain surface remineralization; Depth of valley (red arrow) reduced to <1µm. a3-4- Effective HAC and grain growth with many flat and smooth surfaced HACs; Empty areas below remineralizing front (Red circle). a5- Block shaped HAC on facets of linearly growing grain (red arrows). Rod shaped HAC, deposition and growth (D&G) in depth of valley, reducing its depth to <1µm. a6- Elevation, valleys & effective HAC D &G of different shapes in both areas. Black arrows in a4-6 show correlation in areas.

b1-2- Perpendicular HACs and obliterated spaces. b1-4- The circular, shallow, smooth areas (CSSAs) (red arrows and circles). b5-6- serrated and smooth flat HAC (red and black arrows). Smooth flat HAC are bare with no further precipitation on it. Steps, at edges of these HACs (yellow arrows).c1-3- Effective remineralization (black arrow) with many CSSAs (red arrows). c4-6- Good grain growth in general. Flat HAC showed stacking of crystals from depth in 3D image with formation of steps (yellow arrow-c6). c7-10- Steps on boundary of flat crystals (yellow arrow), with smooth and bare surface. Steps appear like thick lines in c8. Heads of growing rod shaped, perpendicularly oriented HAC seen in c7&8. Black area in c9 is the empty area (red arrow) in c10. c11-12- (yellow rectangle in c10)- No grain growth on flat HAC.

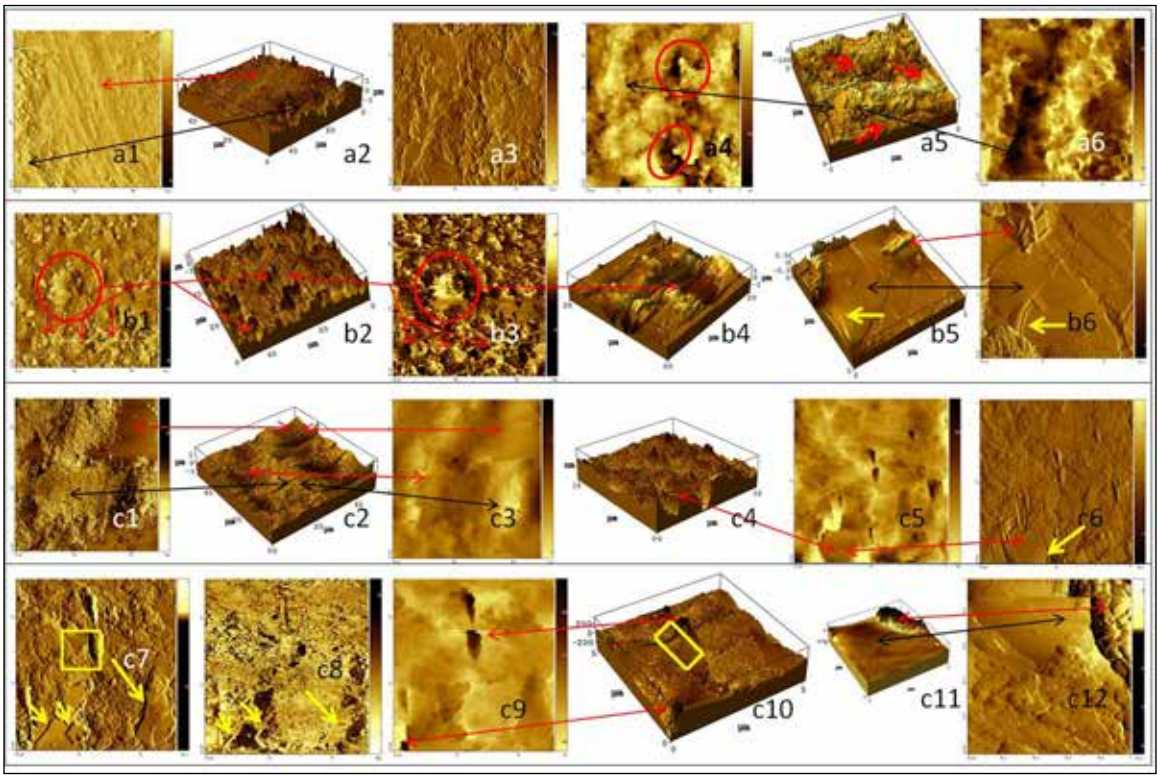

Table 2: Means of roughness average (Ra) of enamel specimens

	N	R_a (µm) Mean	SD	Min	Max
Group I	4	1.3520	0.68172	0.55	2.21
Group II	4	2.2495	0.57010	1.47	2.83
Group III	4	1.6761	0.14380	1.52	1.86
Group IV	4	1.8957	0.56552	1.31	2.66
Group V	4	2.4582	0.14179	2.30	2.65
Total	20	1.9263	0.58822	0.55	2.83

K W ANOVA ; p = 0.058 ; Not Sig

Figure 5(Group V, a-b-c series): All samples showed stair remineralization. a1- general smooth surface and shallow linear valley. a2-5(3D views from various perspectives);a2- remineralization in stair pattern with regular step heights. Horizontal surface of steps are smooth, comprised of linear-parallel & closely packed needle shaped HACs. a3- needle shaped HAC growth. a4- top view- horizontal steps are very smooth, comprised of several grains. a5- lateral view- steps of staired remineralization are <1µm. a6- flat HACs appearing superficially placed (red and black arrows) with adjacent perpendicularly oriented heads of HACs. a7-resolved that superficially appearing one flat crystal is in depth (red arrow) and the other was dome shaped (black arrow). a8- Contrast image- flat HACs appeared black with the immersed needle shaped HACs. All HACs, instead being perpendicular are at angle to it, giving key hole appearance in a6-2D. a9-11- Typical key hole appearance of closely packed HACs with grain growth involving them, seen in a9. Growing grains, meeting at grain boundary, further involving HACs in a10.

b1-2- Smooth and rough area of remineralization. Stair pattern of remineralization, disclosed in 3D. Slanting surface on left and right side are smooth & rough respectively. b3-4- Inclusion of HACs in growing grain upto rough surface boundary or probably the step. Horizontal surfaces of stair has smooth and rough area, each comprised of closely packed, needle shaped & perpendicular HACs. Vertical step in b4 is light shiny area in b5. b6- Growing grain on underlying HACs. b7 (magnified view of yellow rectangle in b3)- Flat HACs with depression in middle. b8- Flat HAC in b6 &7 is covering a big grain in b9, therefore depressed in middle. Multiple steps of flat HAC (black arrow). b10-12- Layers of flat HAC and inclusion of perpendicular HACs within growing grain.

c1-2- Stair pattern remineralization. Perpendicular HACs are as closely stacked plates. Horizontal surfaces are comprised of grains. c3- Smooth and rough areas (black & red arrow). Smooth area comprised of growing grain covering closely packed, plate like HACs. c4(yellow rectangle in c2)- Smooth surface having grain and linear scratches. On right side HACs are closely packed plates. c5- Scratches as light shiny lines suggestive of gaps. Surface showing heads of needle shaped perpendicular HACs. Linear scratches in c4&5 are confirmed as gaps in c6. c7-9- The area in c5&6, appeared granular comprised of heads of needle shaped perpendicular HACs. Smooth areas in c1&2 as closely packed, parallely arranged plates even in c9. c10-11- Two areas of grain growth. c12(3D)- Grains with underlying nano-heads of HACs.

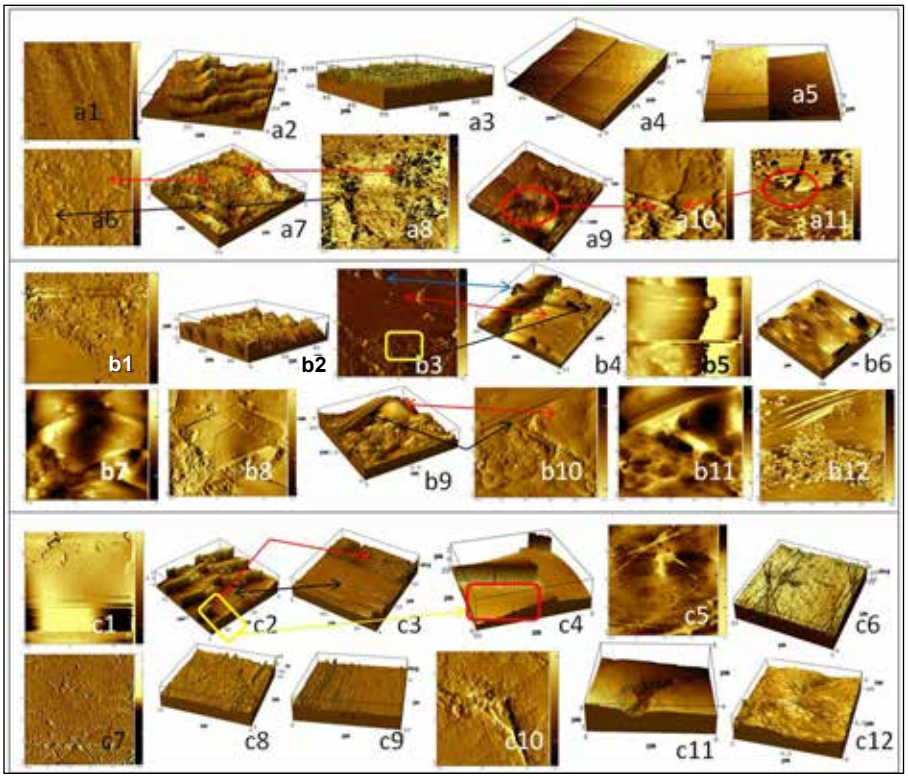

DISCUSSION

To the best of our knowledge, ours is the first study depicting topography of enamel (normal, bleached or treated) depicting deposition and growth (D&G) of HACs. AFM images are described with the help of literature available in dental or other scientific journals.

There being no previous AFM study for normal enamel, mechanism of flat areas in first pattern of group I was not clear (fig 1). Possible explanations may be- a) In height Image (HI) flat HAC showed heads of HACs; reflecting probability of grain with inclusion of closely packed HACs[30]; b) actual flat HAC i.e. 'a' face toward surface; and c) these were crystals of calcium phosphate other than HACs. Morphology of this sample gave rise to the possibility of aprismatic enamel. One prism in third pattern of group I revealed needle shaped HACs i.e. more growth along 'c' axis but less maturation laterally on 'a' or 'b' faces (fig 1, c series).[26] Possibly enamel would clinically present hypomaturation-hypoplastic defect. It is important to note that no defects were detected under stereomicroscope. Polishing of samples would have destroyed these important variations in visibly and stereomicroscopically normal enamel. Some AFM studies observed prisms with flat and even surface in untreated polished samples.[27]

Group-I had the least Ra (1.352µm), similar to El-Halim's[24] AFM study comparing 3 bleaching agents and found least Ra in untreated group.

Severe morphologic alterations, in general, were observed in group II. In first pattern, concentrated H_2O_2 dissoluted matrix in enamel exposing HACs thereby resulting in partial dissolution and opening up of nanospaces within and sides of crystals. Images in a-series perhaps showed bleaching of aprismatic enamel. Plates of HACs were seen, arranged parallel to each other and perpendicular to surface. In second pattern of group II, again, matrix dissolution exposed underlying orientation of HACs within and at periphery of prism (b1-5). Although samples were randomly selected, the AFM topography can be correlated to c-series of figure-1 and explanations about the orientation of HACs there were now clearly visible. Nonetheless severe roughness of bleached enamel was obvious in both patterns.

Table 3: Intergroup comparison of roughness average (Ra)

Mann Whitney Comparison			
Group	**Compared to**	**p Value**	**Significance**
Group I	Group II	0.043	Sig
	Group III	0.248	Not Sig
	Group IV	0.248	Not Sig
	Group V	0.021	Sig
Group II	Group III	0.248	Not Sig
	Group IV	0.386	Not Sig
	Group V	0.564	Not Sig
Group III	Group IV	0.386	Not Sig
	Group V	0.021	Sig
Group IV	Group V	0.248	Not Sig

Compared to 'a' face, 'c' face of HAC is more resistant to acid dissolution.[31, 32] This property of HAC was reflected in AFM images of bleached group i.e. more corrosive picture on aprismatic or interprismatic enamel, while type-II etching pattern was observed within prism similar to McGuckin *et al* [33] Bitter *et al* [34] observed irregular surface grooves on enamel surface bleached with 30% H_2O_2 with associated decrease in Ca/P ratio, even with 15min bleaching exposure which can be related to the severity of enamel surface alterations and increased roughness average in our AFM images (Figure-2, table-2). Our images support the important findings of a TEM study by Lai *et al* [14], who found partial dissolution of heads ('c' face) and band like dissolution on sides ('a' face) of HACs after bleaching.

In general, demineralization of bleached enamel surface is related to the low pH of the product. Though Pola-Office claims neutral pH, litmus paper (Qualigens) test showed it 5, below the critical pH for enamel, similar to many investigators.[35-36] Accordingly bleaching products should have neutral pH to minimize damage of enamel surface.[37] Nonetheless, H_2O_2 remains stable in acidic medium only[37] else it might disproportionate into water and oxygen.[17]

Ra of group-II was the second highest which was significantly different from group-I (unbleached) similar to El-Halim[24] (tables 2&3).

In FT-IR study by Bistey *et al* [12] normal human hydroxyapatite showed carbonate defects in hydroxyapatite lattice. These defects were found replaced with hydroxyl radical ($OH^{\cdot}$) released from H_2O_2 during bleaching.[15-17] Their findings prove that HACs are affected by both H_2O_2 and pH of bleaching product. The enamel surface alterations can therefore become more susceptible for various adverse effects especially where remineralization is not reversed within time as in cases where saliva has lesser ionic product than the solubility product of enamel.[38]

Noticeable but incomplete remineralization was observed in group-III (Figure-3, a-b series). Crystal growth on 'c' face from pre-existing partially dissolved HAC in bleached group was depicted (a4-12). The 'c' face of HAC is negatively charged owing to predominance of phosphate group favoring precipitation of positively charged calcium ions with rapid growth.[31] Apart from intracrystal growth, flat shaped HACs were also found (a4-9, red arrow). Vandiver *et al* [39] studied the nanoscale morphology of HAC onto synthetic hydroxyapatite from simulated body fluids. Similar to our study, they localized three distinct morphologies of HAC including hemispherical, elongated needle-like and the relatively smooth regions of larger, irregularly shaped structures. They explained this phenomenon as different facets or grains on the initial HA surface would have different exposed crystal planes and therefore differing solubility, which have influence on the structure, morphology, and composition of the precipitated apatite layer. In consecutive study, they[40] described the same- 'as the surface charge varies with nanoscale position on apatite surface, it is most likely associated with exposed crystal planes and accordingly expected surface charge to have a strong influence on the process of

organic and inorganic deposition and structural evolution on the nucleating material'. Furthermore, remineralization inhibition might also be due to the presence of oxygen bubbles in deeper layers[14] or due to the attached ROS on HAC lattice.[12]

Increased microhardness after immersion of bleached samples in saliva by Basting *et al.*[41] could be correlated to the partial remineralization as seen in our AFM images. Similar to our study, many studies found reversal of erosive surface defects of bleaching following saliva immersion of bleached samples.[13, 42] Contrary to these, Borges *et al* [43] and Rodrigues[44] did not observe significant difference in microhardness of bleached enamel or bleached+saliva group perhaps owing to unfavorable orientation of HACs on enamel samples to start with or had microindentations on interprismatic area as in both conditions enamel would have lesser microhardness. Viswanath *et al* [45] observed mechanical behavior of single HAC through nano- and microindentation on prism and basal planes and found that 'c' facet (basal plane) orientation was stiff and hard as compared to 'a' facet (prism faces) showing its strong anisotropic behavior and also that microindentation (contrary to nanoindentation) was always associated with cracks or fracture of HAC. These differences in observations of various micro and nanoscopic studies emphasize the need of more descriptive baseline nanoscopic studies for in-depth understanding of de- and remineralization phenomenon of enamel.

Ra of group-III was significantly less to group-V (table-3). El Halim *et al* [24] had not disclosed immersion medium of bleached samples. Our AFM study may be the first to observe the effect of saliva on bleached enamel.

Incomplete remineralization, as observed in our study and partial recovery of bond strength, perhaps are the two depictions of same underlying phenomenon *i.e.* presence of ROS on bleached surface which hampers both remineralization and polymerization of composites. It is proven that immediate antioxidant application after bleaching increase the bond strength.[14, 18, 20] Therefore we probed the effects of two antioxidants, catalase and SA, on the topography of bleached enamel.

AFM images of group IV showed not only effective increase in width and thickness of partially dissolved HAC in all patterns but also new HAC deposition thereby giving rise to vivid patterns of remineralization. Block shaped HACs (effective remineralization on all three faces[26] of HAC) deposited on elevated parts as well as in valleys (figure-4, a4-6). Linear remineralization was perhaps due to bleached aprismatic enamel being the nucleating surface. In b-series of this group, perhaps the main area of rapid remineralization was prismatic surface as interprismatic lines of parallel oriented HACs was visible similar to figure-2, b-series. Smooth plates were the precipitation of flat HACs in multiple layers (b5-6); some having steps at edges (yellow arrows, b5-6). Despite polycrystalline remineralization in c-series, thickness of individual HACs was lesser than that of a-series, where block shaped HACs were found. Nonetheless HACs were closely packed with good grain growth (c3-12). Similar to b-series of this group, flat HACs had steps here too, reflecting their inherent property. Finding of empty spaces below growing HACs (red circles, a4) and CSSA in other two samples proved gas formation (oxygen) at subsurface. A vent for its escape was also observed (red arrows, c9-10). Probably CSSAs were the impressions of bottom surfaces of escaped oxygen bubbles. We assume that the Haber-Weiss cycle (detoxifying of H_2O_2 into water and oxygen by catalase)[46] took place inside bleached enamel with oxygen, slowly escaping through growing grains on surface.

Ra of group IV was non-significantly lesser(groups II & V) or higher (groups I & III)(table-3). Reduced Ra reflected relative smoothness of remineralized enamel surface.

The antioxidant sodium ascorbate also potentiated remineralization with D&G of HACs but in quite different pattern. Here the HACs' growth was along 'c' axis with closed stacking in stair-pattern. Even heighted, closely packed needle shaped with good grain growth gave rise to smooth horizontal surface of a stair.

Ra of group V was highest among all groups and significantly different from group III and even group I (table-3), probably due to the difference in type and pattern of deposited HACs *i.e.* block shaped with even pattern in catalase and needle shaped with stair-pattern in sodium ascorbate group.

Antioxidants potentiated its effect perhaps by neutralizing the remaining molecules of ROS [H_2O_2 by catalase[45]; $OH^{\cdot}$ by SA[48]]. This difference in mechanism of action of two antioxidants may be the reason for different patterns of remineralization. Bistey *et al* [12] observed that $OH^{\cdot}$ from oxidative bleaching agents replaced the naturally present carbonate defects in HAC lattice. Stairs type pattern of remineralization after SA application does not meet his explanation. Carbonate defect are randomly present[26] rather than regularly on highly oriented HACs.[49] Secondly carbonate defects are more abundant near DEJ.[26] We assume that some other mechanism also exists along with Bistey's finding of carbonate defects, needing further research.

Evident but incomplete remineralization in group-III support Garcia *et al* [50] who studied the antioxidant activity of saliva, SA and catalase with DPPH- a free radical assay. They graded catalase and saliva having intermediate while SA as high antioxidant activity. Our images contradict their findings. This difference is because of the mechanism of the DPPH free radical assay, which is based on electron transfer and as SA has affinity for $OH^{\cdot}$ radical,[48] could effectively bond with DPPH. On the other hand catalase enzyme reacts with whole molecule of H_2O_2, with no affinity for oxidative radicals did not react with DPPH, thereby affecting their results. On the contrary, in some studies catalase resulted better bond strength compared to SA. [19] Different pattern of D&G of HACs in two tested antioxidants in this study may be the reason of difference in bond strength. Kum *et al* [51] studied the bond strength after applying catalase, 70% ethanol or sprayed water and found catalase significantly superior to the other two. In their study too, 70% ethanol was $OH^{\cdot}$ scavenger[46], similar to sodium ascorbate in our study & thereby reflected similarity with our results. Nonetheless both antioxidant groups showed faster remineralization as

compared to the saliva group in our study, proving remineralization potentiation by saliva is directly proportional to ROS neutralization by any agent capable of doing so.

According to the literature available, formation of flat HACs ('100' or 'a' surface) with steps at edges is not kinetically favorable for consecutive acid attacks.[25] Kwon *et al* [25] stated that the characterization of HAC surfaces on the molecular level is important for achieving a fundamental understanding of dental caries processes. They found that molecular steps on '100' face parallel to the elongated axes of HACs are not only energetically favorable but also kinetically dominant under dissolution conditions. Further studies are required to validate this statement.

When we probe the overall results of various studies regarding dental bleaching, we cannot deny the effect of antioxidants be it mild (saliva), moderate (antioxidant affinity for radicals) or potent (catalase, affinity for H_2O_2). Our AFM images suggest saliva induces healing of partially dissoluted HACs, while SA and catalase stimulated faster precipitation of HACs on them. That we have not studied the depth of enamel lesions is the limitation of our study. Molecular studies together with depth images of enamel and dentine are required to understand the reversal of bleaching effect.

CONCLUSIONS

Within the limitation of this study we conclude that 35% H_2O_2 in-office bleach produced severe surface irregularities. Artificial saliva remineralized the bleached enamel primarily by crystal growth of pre-existing partially dissoluted HACs. Both SA and catalase potentiated the remineralizing ability of saliva but none returned the original topography of bleached enamel. Catalase application resulted in generalized smoother pattern of remineralization whereas stair-pattern remineralization was seen following SA. Moreover catalase favored D&G of rod and block shaped HACs whereas SA, the needle shaped HACs of uniform heights with 'c' face towards enamel surface.

Based on conclusions of this study application of antioxidant is recommended after each session of in-office bleaching. This study also expanded the use of AFM in dentistry, beyond the evaluation of surface roughness, and proved it as a powerful tool to probe surface topography effectively. As the observation of the biological crystals is of prime importance for studying the calcification mechanisms (crystal growth), biological properties and destructive phenomena of calcified tissues (i.e., dental caries and bone resorption), this study will provide a useful basis for future work.

We are thankful to Mr. Kinny Pandey, Research associate, Department of Chemistry, Indian Institute of Technology, Indore, India for his help for AFM work.

REFERENCES

1. Haywood VB. History, safety, and effectiveness of current bleaching techniques and applications of the nightguard vital bleaching technique. Quintessence Int 1992;23:471-88.
2. Donly KJ, Donly AS, Baharloo L, Rojas-Candelas E, Garcia-Godoy F, Zhou X, Gerlach RW.
Tooth whitening in children. Compend Contin Educ Dent 2002;23(1A):22-8.
3. Leonard RH, Haywood V B, Phillips C . Risk factors for developing tooth sensitivity and gingival irritation associated with nightguard vital bleaching. Quintessence Int 1997;28:527-34.
4. Gursoy UK, Eren DI, Bektas OO, Hurmuzlu F, Bostanci V, Ozdemir H. Effect of external tooth
bleaching on dental plaque accumulation and tooth discoloration. Med Oral Patol Oral Cir Bucal 2008;13(4):E266-9.
5. Pretty IA, Ellwood RP, Brunton PA, Aminian A. Vital tooth bleaching in dental practice:
Professional bleaching. Dent Update 2006;33(5):288-90.
6. Miranda CB, Pagani C, Benetti AR, Matuda FS. Evaluation of the bleached human enamel
by scanning electron microscopy. J Appl Oral Sci 2005;13(2):204-11.
7. Pinto CF, Oliveira R, Cavalli V, Giannini M. Peroxide bleaching agent effects on enamel surface microhardness, roughness and morphology. Braz Oral Res 2004;18(4):306-11.
8. Ernst CP, Marroquin BB, Zönnchen BW. Effects of hydrogen peroxide-containing bleaching agents on the morphology of human enamel. Quintessence Int 1996;27:53-6.
9. Efeoglu N,Wood D, Efeoglu C. Microcomputerised tomography evaluation of 10% carbamide peroxide applied to enamel. J Dent 2005;33(7):561-7.
10. Camargo SE, Valera MC, Camargo CH, Gasparoto Mancini MN, Menezes MM. Penetration of 38% hydrogen peroxide into the pulp chamber in bovine and human teeth submitted to office bleach technique. J Endod 2007;33(9):1074-7.
11. Ubaldini ALM, Baesso ML, Neto M, Sato F, Bento. Hydrogen peroxide diffusion dynamics on dental tissues. J Dent Res 2013;92:661-65.
12. Bistey T, Nagy IP, Simo A, Hegedus C. In vitro FT-IR study of the effects of hydrogen peroxide on superficial tooth enamel. J Dent 2007;35:325–30.
13. Oltu U, Gürgan S . Effects of three concentrations of carbamide peroxide on the structure of enamel. J Oral Rehabil 2000;27:332-40.
14. Lai S C N, Tay F R, Cheung G S P, Mak Y F, Carvalho R M, Wei S H Y, Pashley D H. Reversal of compromised bonding in bleached enamel. J Dent Res 2002;81(7):477-81.
15. Dahltrom SW, Heithersay GS, Bridges TE. Hydroxyl radical activity in thermo-catalytically bleached root- filled teeth. Endod Dent Traumatol 1997;13:119-25.
16.Tanaka MK, Tsujimoto Y, Kawamoto K , Senda N, Ito K, Yamazaki M. Generation of free radicals and/or active oxygen by light or laser irradiation of hydrogen peroxide or sodium hypochlorite. J Endod 2003;29(2):141-43.
17. Sharma DS, Sharma S, Natu SM, Chandra S. An in vitro evaluation of radicular penetration of hydrogen peroxide from bleaching agents during intra-coronal tooth bleaching with an insight of biologic response. J Clin Pediatr Dent 2011 Spring;35(3):289-94.
18. Bulut H, Turkun M, Kaya A D. Effect of an antioxidizing agent on the shear bond strength of brackets bonded to bleached human enamel. Am J Orthod Dentofacial Orthop 2006;129(2):266-72.
19. Torres CRG, Koga AF, Borges AB. The effects of anti-oxidant agents as neutralizers of bleaching agents on enamel bond strength. Braz J Oral Sci 2006;5(16):971-76.
20. Kaya AD, Türkün M, Arici M. Reversal of compromised bonding in bleached enamel using antioxidant gel. Oper Dent 2008;33(4):441-47.
21. Dishman MV, Covey DA, Baughan LW. The effects of peroxide bleaching on composite to enamel bond strength. Dent Mater 1994;10(1):33-6.
22. McGuckin RS, Thurmond BA, Osovitz S. Enamel shear bond strengths after vital bleaching. Am J Dent 1992;5:216-22.
23. Hegedüs C, Bistey T, Flóra-Nagy E, Keszthelyi G, Jenei A. An atomic force microscopy study on the effect of bleaching agents on enamel surface. J Dent 1999;27(7):509-15.
24. El Halim SAMA. Effect of three bleaching agent on surface roughness of enamel (in-vivo study). Dentistry 2012;2(4):1-5.

25. Poggio C, Lombardini M, Colombo M, Bianchi S. Impact of two toothpastes on repairing enamel erosion produced by a soft drink: An AFM in vitro study. J Dent 2010;38:868-74.
26. Kwon KY, Wang E, Chang E, Lee SW. Characterization of the dominant molecular step orientations on hydroxyapatite (100) surfaces. Langmuir 2009;25(13):7205-208.
27. Simmer JP, Fincham AG. Molecular mechanisms of dental enamel formation. Crit Rev Oral Biol Med 1995;6(2):84-108.
28. Francescut P, Zimmerli B, Lussi A. Influence of different storage methods on laser fluorescence values: a two year study. Caries Res 2006;40:181-85.
29. Hicks MJ, Flaitz CM. Enamel caries formation and lesion progression with a fluoride dentifrice and a calcium phosphate containing fluoride dentifrice: A polarized light microscopic study. ASDC J Dent Child 2000;67(1):21-8.
30. Grain growth available from http://en.wikipedia.org/wiki/Grain_growth (downloaded on 7th April 2014).
31. Hagio T, Tanase T, Akiyama J, Iwai K, Asai S. Different properties exhibited on the two typical crystal faces of hydroxyapatite in a simulated body environment. Journal of Physics: Conference Series 156 (2009);012004:1-7.
32. Kim HM, Himeno T, Kokubo T, Nakamura T. Process and kinetics of bone-like apatite formation on sintered hydroxyapatite in a simulated body fluid. Biomaterials 2005;26(21):4366-73.
33. McGuckin RS, Babin JF, Meyer BJ. Alterations in human enamel surface morphology following vital bleaching. J Prosthet Dent 1992;68(5):754-60.
34. Bitter NC, Sanders JL. The effect of four bleaching agents on the enamel surface; A scanning electron microscopic study. Quintessence Int 1993;24:817-24.
35. Batista GR, Pagani C, Borges AB , Pucci CR , Torres CRG. Evaluation of Dental Bleaching Gels' pH in Enamel Contact . International Journal of Contemporary Dentistry 2010;1(1):1-5.
36. Freire A, Archegas LR, de Souza EM, Vieira S. Effect of storage temperature on pH of in-office and at-home dental bleaching agents. Acta Odontol Latinoam 2009;22(1):27-31.
37. Price RBT, Sedarous M, Hiltz GS. The pH of tooth-whitening products. J Can Dent Assoc 2000;66:421-6.
38. Dawes C. What is the critical pH and why does a tooth dissolve in acid? J Can Dent Assoc 2003;69(11):722-4
39. Vandiver J, Patel N, Bonfield W, Ortiz C. Nanoscale morphology of apatite precipitated onto synthetic hydroxyapatite from simulated body fluid. Key Engineering Materials 2005;284:497-500.
40. Vandiver J, Dean D, Patel N, Bonfield W, Ortiz C. Nanoscale variations in surface charge of synthetic hydroxyapatite detected by chemically and spatially specific high resolution force spectroscopy. Biomaterials 2005;26:271-83.
41. Basting RT, Rodrigues Jr. AL, Serra MC. Effects of seven carbamide peroxide bleaching agents on enamel microhardness at different time intervals. J Am Dent Assoc 2003;134:1335–42.
42. Tu¨rku¨n M, Sevgican F, Pehlivan Y, Aktener BO. Effects of 10% carbamide peroxide on the enamel surface morphology: a scanning electron microscopy study. J Esthet Restor Dent 2002;14:238–44.
43. Borges AB, Yui KCK, D'Avila TC, Takahashi CL, Torres CRG, Borges ALS. Influence of remineralizing gels on bleached enamel microhardness in different time intervals. Oper Dent 2010;35(2):180-86.
44. Rodrigues JA, Marchi GM, Ambrosano G, Heymann HO, Pimenta LA. Microhardness evaluation of in situ vital bleaching on human dental enamel using a novel study design. Dental Materials 2005;21(11):1059-67.
45. Vishwanath B, Raghavan R, Ramamurthy U, Ravishankar N. Mechanical properties and anisotrophy in hydroxyapatite single crystals. Scripta Materialia 2007;57:361-64.
46. Imlay JA, Chin SM, Linn S. Toxic DNA damage by hydrogen peroxide through Fenton reactions in vivo and in-vitro. Science 1988;240(4852):640-2.
47. Bowles WH, Ugwuneri Z. Pulp chamber penetration by hydrogen peroxide following vital bleaching procedures. **J Endod** 1987;13(8):375-77.
48. Oskoee PA, Navimipour EJ, Oskoee SS , Moosavi N. Effect of 10% sodium ascorbate on bleached bovine enamel surface morphology and microhardness. Open Dent 2010;4:207-10.
49. Tsuda H, Arends J. Orientational micro-raman spectroscopy on hydroxyapatite single crystals and human enamel crystallites. J Dent Res 1994;73(11):1703-10.
50. Garcia EJ, Oldoni TL, Alencar SM, Reis A, Loguercio AD, Grande RH. Antioxidant activity by DPPH assay of potential solutions to be applied on bleached teeth. Braz Dent J 2012;23(1):22-7.
51. Kum KY, Lim KR, Lee CY, Park KH, Safavi KE, Fouad AF, Spångberg LS. Effects of removing residual peroxide and other oxygen radicals on the shear bond strength and failure modes at resin-tooth interface after tooth bleaching. Am J Dent 2004;17(4):267-70.